International Journal of Multiphase Flow 36 (2010) 333–348

Contents lists available at ScienceDirect

International Journal of Multiphase Flow

journal homepage: www.elsevier.com/locate/ijmulflow

A coupled model for simulation of the gas–liquid two-phase flow with complex flow patterns

Kai Yan, Defu Che *

State Key Laboratory of Multiphase Flow in Power Engineering, Xi'an Jiaotong University, Xi'an 710049, China

ARTICLE INFO

Article history:
Received 2 July 2009
Received in revised form 10 November 2009
Accepted 16 November 2009
Available online 20 November 2009

Keywords:
Interface tracking
Two-fluid model
MCBA–SIMPLE
Length scale
Gas–liquid two-phase flow
Volume fraction redistribution
Complex flow patterns

ABSTRACT

A new model coupling two basic models, the model based on interface tracking method and the two-fluid model, for simulating gas–liquid two-phase flow is presented. The new model can be used to simulate complex multiphase flow in which both large-length-scale interface and small-length-scale gas–liquid interface coexist. By the physical state and the length scale of interface, three phases are divided, including the liquid phase, the large-length-scale-interface phase (LSI phase) and the small-length-scale-interface phase (SSI phase). A unified solution framework shared by the two basic models is built, which makes it convenient to perform the solution process. Based on the unified solution framework, the modified MCBA–SIMPLE algorithm is employed to solve the Navier–Stokes equations for the proposed model. A special treatment called "volume fraction redistribution" is adopted for the special grids containing all three phases. Another treatment is proposed for the advection of large-length-scale interface when some portion of SSI phase coalesces into LSI phase. The movement of the large-length-scale interface is evaluated using VOF/PLIC method. The proposed model is equivalent to the two-fluid model in the zone where only the liquid phase and the SSI phase are present and to the model based on interface tracking method in the zone where only the liquid phase and the LSI phase are present. The characteristics of the proposed model are shown by four problems.

1. Introduction

Gas–liquid two-phase flow plays an important role in many natural and industrial processes such as chemical engineering, nuclear engineering and multiphase transportation and so on (Wallis, 1969; Ishii and Zuber, 1979). Gas–liquid two-phase flow contains various flow patterns, which have great influences on hydrodynamics, heat transfer and mass transfer. Due to the limited understanding on the phenomenon of gas–liquid two-phase flow, there is an urgent need for a better insight into the details of this flow. Computational fluid dynamics (CFD) is a good tool for simulating gas–liquid two-phase flow. One of the main merits of CFD is that it can make an in-depth understanding of the underlying physical mechanisms. Besides, it can also provide the distributions of flow-related parameters for engineering applications. The special computational models and methods are usually developed for the individual flow pattern of gas–liquid two-phase flow. In this paper, flow patterns are classified by the length scale of interface, which differs from the conventional flow pattern classification.

The model based on interface tracking method is one of the basic two-phase models. This model is suitable for the flows with large-length-scale gas–liquid interface, where the length scale of interface is usually much larger than that of computational grid so that the movement and deformation of interface can be taken into account in numerical simulation. In this model, the interface tracking method, which keeps the interface sharp and enables the accurate location of transient interface when interface advects, is applied in combination with the Navier–Stokes equations.

At present, there are several types of interface tracking methods. The volume of fluid (VOF) method (Hirt and Nichols, 1981) and the Level Set method (Sethian, 1998), which employ a static grid system, are popular in the simulation of two-phase flow with large-length-scale interface. These two methods have been applied to a variety of two-phase flow problems (Olsson and Kreiss, 2005; Zheng et al., 2007). The front tracking methods (Gardner et al., 1988; Unverdi and Tryggvason, 1992) determine the location of interface in an explicit way. In these methods, markers are distributed evenly near the interface, and then are propagated. The markers may however move close to or apart from each other. Hence, the redistribution of markers is needed. The marker-and-cell method (MAC). (Harlow and Welch, 1965) is one of the interface tracking methods using Lagrangian approach. Massless particles are introduced to locate the interface in the Lagrangian manner. For the Arbitrary Lagrangian Eulerian method (ALE) (Hirt et al., 1974; Hughes et al., 1981), the interface is considered to be one of the

* Corresponding author. Tel.: +86 29 82665185; fax: +86 29 82668703.
E-mail address: dfche@mail.xjtu.edu.cn (D. Che).

0301-9322/$ - see front matter © 2009 Elsevier Ltd. All rights reserved.
doi:10.1016/j.ijmultiphaseflow.2009.11.007

boundaries of the grid system and the grids deform as the interface moves. A good grid moving algorithm is necessary to deal with moving boundaries.

If the length scale of interface is very small or equivalent to that of computational grid, where the length scale of interface is smaller than the minimal length scale needed to locate the interface, the accurate location of the interface cannot be obtained by the model based on interface tracking method and the result will lose its physical meaning. It is obvious that a new approach is necessary.

The two-fluid model (Ishii, 1975) was thus developed for simulating the small-length-scale bubbles, such as bubbly or dispersed flow. For this flow pattern, the averaged parameters are usually concerned. In the two-fluid model, each phase has its corresponding set of governing equations, including the continuity equation, the momentum equations and the energy equation. The averaged governing equations, not the original ones, are used to solve the two-phase flow problem. Various averaging methods have been proposed, such as time averaging, spatial averaging and ensemble averaging (Drew, 1983; Bruce and Wendroff, 1984; Zhang and Prosperetti, 1994). The lack of closure relationship is considered to be the weakness of all the averaged governing equations. However, it is not an obstacle to the wide application of the two-fluid model to two-phase flow problems.

Over the past several decades, many progresses have been made for the model based on interface tracking method and the two-fluid model, which are two basic models for simulation of gas–liquid two-phase flow. The two basic models have been developed for specified flow patterns. The model based on interface tracking method is suitable for the flow with large-length-scale interface, and the two-fluid model for the flow with small-length-scale interface. However, under real gas–liquid flow conditions, the interfaces with various length scales usually coexist. Neither of the two basic models is enough for real flow conditions. Obviously, the model for the simulation of real gas–liquid flow must have all the characteristics of the two basic models. One choice is to directly couple the two basic models. However, in the process of coupling, an intrinsic difficulty must be faced, that is, the solution frameworks for the two basic models are different. In the model based on interface tracking method, two phases share one velocity field, which is obtained by solving one set of momentum equations. In the two-fluid model, the velocity fields of two phases are obtained by solving the respective momentum equations. Whether the velocity fields are shared or not results in the difference in solution framework. This just raises an obstacle when coupling the two models. Besides this, the description of the volume fraction is another trouble in coupling. The interface tracking methods are developed specially for sharp interface and less diffusion. However, in the two-fluid model, the solution of volume fraction emphasizes on the effect of averaging. The two different emphases on volume fraction is also a block needed to be removed when coupled into one model.

Some researchers have paid attention to these difficulties and dedicated their efforts to resolve them Anglart and Podowski (2002) derived a modified two-fluid model for fully developed slug flow with time averaging in the period of a Taylor bubble moving through a whole slug cell. A novel time averaging method was introduced to characterize periodical slug flow, which greatly differs from conventional averaging methods, such as those mentioned above. The corresponding closure relationships were developed specially for periodic slug flow. However, it is hard to deal with the flow patterns other than periodic slug flow, such as the developing slug flow or the flow of a Taylor bubble followed by a column of small bubbles Cerne et al. (2001) coupled the VOF method as the interface tracking method with the two-fluid model. The coupled model has been used for the simulation of the two-phase flow with the dispersion of the interface. The VOF method was used in the part of the computational domain where the grid density allowed interface tracking, while in the part of the domain where the interface was too dispersed to be described by the interface tracking algorithms, the two-fluid model was used. The criterion based on the estimation of the local dispersion of interface in the cell was constructed to switch the two models. In the criterion, a dispersion function was introduced to achieve the switch by comparing its value with a threshold value. However, the selection of the threshold value had an influence on the accuracy of calculation. In their model the coupling of the two models was realized by switch but not by a uniform framework. In essence, this model is not a genuine coupled model. Moreover, the characteristics of the gas–liquid two-phase flow have not been included in their so-called coupled model.

Despite some progresses, it is obvious that there is still a long way to enable the simulation of real gas–liquid flows. Therefore, it is an urgent need and a challenging work to develop a new model for gas–liquid two-phase flow with complex flow patterns where small and large-length-scale interfaces coexist. In this paper, a new model is developed by coupling the model based on interface tracking method and the two-fluid model for simulation of incompressible gas–liquid two-phase flow. The Navier–Stokes equations are rearranged based on a unified solution framework and are solved by the MCBA–SIMPLE algorithm. The special treatment called "volume fraction redistribution" is employed to deal with the zones containing both small and large-length-scale interfaces. Four problems are provided to show the characteristics of the new coupled model.

2. Conventional models for simulation of two-phase flow

2.1. The model based on interface tracking method

The model based on interface tracking method, in which the movement of large-length-scale interface is considered, has been developed to simulate two-phase flow. The interface tracking methods include VOF, MAC, Level Set, etc., which are developed specially for the advection of interface. The essence of these methods is to keep the interface sharp, which allows the accurate location of interface and the simulation of surface phenomenon. The model based on interface tracking method can be used to describe gas–liquid two-phase problems of some special flow patterns, such as the stratified flow in horizontal tubes and the slug flow in vertical tubes, etc., where the length scale of gas–liquid interface is much larger than the grid size. In this model, the two phases share one set of continuity and momentum equations. For the systems of incompressible viscous two-phase flow, the following continuity and momentum equations are usually used (Puckett et al., 1997).

$$\begin{aligned} &\nabla\cdot\vec{\boldsymbol{U}}=0\\ &\rho\frac{\partial\vec{\boldsymbol{U}}}{\partial t}+\rho\nabla\cdot(\vec{\boldsymbol{U}}\,\vec{\boldsymbol{U}})=-\nabla p+\nabla\cdot(\mu\underline{\vec{\boldsymbol{D}}})+\vec{\boldsymbol{M}}+\rho\vec{\boldsymbol{g}} \end{aligned} \tag{1}$$

where $\vec{\boldsymbol{U}}$ is velocity vector, p is pressure, $\underline{\vec{\boldsymbol{D}}}=\frac{(\nabla\vec{\boldsymbol{U}}+\nabla\vec{\boldsymbol{U}}^T)}{2}$, $\vec{M}$ represents momentum exchange term, e.g. surface tension force and $\vec{\boldsymbol{g}}$ is the gravitational acceleration. The density ρ and the viscosity μ, shared by the two fluids, are the functions of space and time.

For the interface tracking methods, the advection equation for interface is employed in the following form (Puckett et al., 1997):

$$\frac{\partial f}{\partial t}+\vec{\boldsymbol{U}}\cdot\nabla f=0 \tag{2}$$

where f denotes the indicator of the location of interface, which has different meanings for different interface tracking methods. The

indicator f is also used to calculate the fluid properties, e.g., density and viscosity, at grid points.

$$\begin{aligned}\rho &= f\rho_1 + (1-f)\rho_2 \\ \mu &= f\mu_1 + (1-f)\mu_2\end{aligned} \tag{3}$$

Since the main goal of this paper is to develop the model coupling the model based on interface tracking method and the two-fluid model, it is essential to select an appropriate interface tracking method for the new model.

2.2. The two-fluid model

The two-fluid model is one of the basic numerical models for multiphase flow. It is usually applied to the two-phase flow such as bubbly flow or dispersed flow, where the length scale of the gas–liquid interface is smaller or equivalent to the grid size and only the averaged effects of physical variables are concerned. In the model, each phase, which occupies the whole space, is considered as continuous fluid.

The governing equations of this model pioneered by Wallis (1969), Drew and Lahey (1982) and Ishii and Mishima (1984) were derived by averaging the original ones for single phase fluid. There are several averaging methods including time, space, ensemble averaging, etc. Two sets of governing equations govern the conservations of mass, momentum, and energy of each phase. The continuity and momentum equations, developed by Drew and Passman (1998), for the systems of incompressible fluids in the model are given by

$$\begin{aligned}&\frac{\partial}{\partial t}(\alpha_k\rho_k) + \nabla\cdot(\alpha_k\rho_k\vec{\boldsymbol{U}}_k) = 0 \\ &\frac{\partial(\alpha_k\rho_k\vec{\boldsymbol{U}}_k)}{\partial t} + \nabla\cdot(\alpha_k\rho_k\vec{\boldsymbol{U}}_k\vec{\boldsymbol{U}}_k) = -\alpha_k\nabla p + \nabla\cdot(\alpha_k\mu_k\underline{\boldsymbol{D}}_k) + \vec{\boldsymbol{M}}_k + \alpha_k\rho_k\vec{\boldsymbol{g}}\end{aligned} \tag{4}$$

where α denotes the volume fraction. The notation k is the phase indicator with $k = 1$ for phase 1 and $k = 2$ for phase 2. Both fluids share the same space and pressure and have different velocity fields.

Since the averaged variables of one phase are dependent upon the other phase, the interactions between phases are embodied through the source terms of the momentum equations or other scalar equations. In the process of averaging, some information of the interactions between phases is lost, which is compensated usually by more accurate closure relationships provided mostly by experiments as the source terms. The closure relationships are the main source of the uncertainty of the two-fluid model.

3. MCBA–Simple algorithm

Darwish et al. (2001) has developed new multiphase flow algorithms, which fully extended the segregated class of algorithms and many other techniques developed for single-fluid flow to the simulation of multiphase flow. These algorithms fall in two categories, i.e., mass conservation-based algorithms (MCBA) and geometric conservation-based algorithms (GCBA), which depends on that the mass conservation equation or the geometric conservation equation is chosen to derive the pressure equation.

MCBA–SIMPLE algorithm (Darwish et al., 2001) is the SIMPLE algorithm combined with MCBA. The algorithm is very similar to that of original SIMPLE algorithm. The most significant difference is the derivation of the pressure-correction equation (see Appendix A for the detailed derivation process).

Due to limited space, only the solution procedure of MCBA–SIMPLE (Moukalled et al., 2003) is shown as follows:

(1) Solve the individual momentum equations for velocities.
(2) Solve the pressure correction equation based on global mass conservation.
(3) Correct velocities and pressure.
(4) Solve the individual mass conservation equations for volume fractions.
(5) Solve the other scalar equations.
(6) Return to the first step and repeat until convergence.

4. The coupled model

For real flows, large-length-scale bubbles and small-length-scale bubbles, all relative to grid size, are often present simultaneously. Obviously, it is impossible to simulate this kind of flow only with the model based on interface tracking method or with the two-fluid model. The only feasible way is to develop a new method which can simulate the movement of the interfaces with large length scale and the averaged properties of each phase in dispersed flow regions. In other words, the developed model should contain the advantages of the two basic models. Therefore, the main work of this paper is to develop a new coupled model which can simulate the gas–liquid two-phase flow simultaneously containing both small and large-length-scale gas–liquid interfaces.

For the gas–liquid two-phase flow, all fluids, in general, are physically divided into two phases: the liquid phase and the gas phase. However, in the coupled model, there are three phases divided not only by the physical state but also by the length scale of interface, including the liquid phase, the large-length-scale-interface phase (LSI phase) and the small-length-scale-interface phase (SSI phase). Here "large-length-scale-interface" means that the length scale of interface is much larger than grid size so that its movement must be considered, and "small-length-scale-interface" means that the length scale of interface is equivalent to or smaller than grid size so that accurate location of interface cannot be obtained in the grid system or that the averaged effects of physical parameters are concerned in this zone. Corresponding to gas–liquid two-phase flow, the liquid phase stands for the continuous liquid, the LSI phase stands for the bubbles with large length scale interfaces, i.e., large bubbles and the SSI phase stands for the small-length-scale-interface bubble swarms, e.g., dispersed bubbles, respectively. The sketch map of practical gas–liquid flow with the three phases is shown in Fig. 1a.

In the coupled model, the three phases have complicated interactions among them. There are frictional forces on the liquid phase and the LSI phase, i.e., the large-length-scale interface between liquid phase and gas phase, for instance, the frictional force on the liquid at the interface of liquid and the Taylor bubble in slug flow. Breakups and coalescences happen between the LSI phase and the SSI phase. Breakups mean that part of the large bubble near the interface is forced to shake off from the LSI phase and becomes dispersed bubbles due to intensely turbulent disturbances acting on the liquid near the interface. Oppositely, coalescences happen when some gas of the SSI phase catches up with the gas of the LSI phase and enters it. There are also interactions between the liquid phase and the SSI phase. The interactions contain more than one kind of force. In gas–liquid bubbly flow, the interaction consists of drag force, virtual mass force, Basset force, lift force, wall force, and so on. The interactions between one phase and another are shown in Fig. 2.

4.1. The equivalence of two basic models

In the model based on interface tracking method, the continuity and momentum equations for the incompressible viscous gas–liquid fluids are shown as Eq. (1).

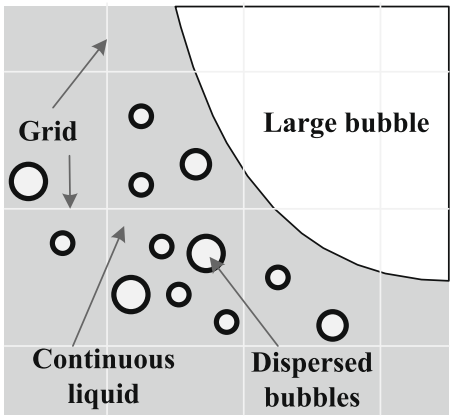

(a)

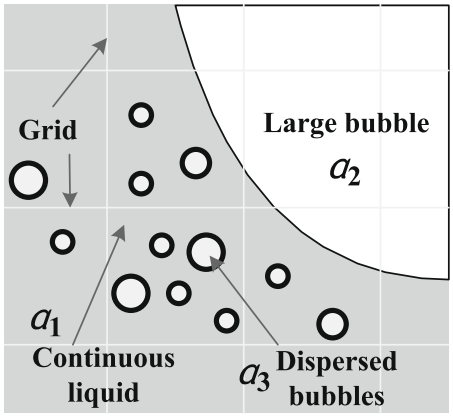

(b)

Fig. 1. Schematic map of three phases divided in the proposed model.

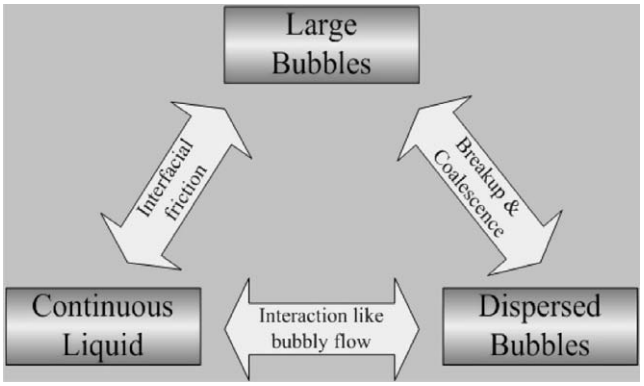

Fig. 2. Interactions among three phases.

Assume that there are two phases in the flow system. With the geometric conservation equation of $\alpha_1 + \alpha_2 = 1$, the continuity equation in Eq. (1) can be rewritten as

$$\nabla \cdot (\alpha_1 \vec{\boldsymbol{U}} + \alpha_2 \vec{\boldsymbol{U}}) = 0,$$

then

$$\frac{\partial}{\partial t}(\alpha_1 + \alpha_2) + \nabla \cdot (\alpha_1 \vec{\boldsymbol{U}} + \alpha_2 \vec{\boldsymbol{U}}) = 0. \tag{5}$$

Considering the interface advection equation $\frac{\partial \alpha_k}{\partial t} + \vec{\boldsymbol{U}} \nabla \cdot \alpha_k = 0$, which will be derived in Section 4.6, the above equation can be split into two equations as follows:

$$\begin{aligned} &\frac{\partial \alpha_1}{\partial t} + \nabla \cdot (\alpha_1 \vec{\boldsymbol{U}}) = 0 \\ &\frac{\partial \alpha_2}{\partial t} + \nabla \cdot (\alpha_2 \vec{\boldsymbol{U}}) = 0. \end{aligned} \tag{6}$$

For incompressible fluids, the above equations have the same form as the continuity equation in the two-fluid model. One of the difference is that the two phases share the same velocity field, i.e., $\vec{\boldsymbol{U}}_1 = \vec{\boldsymbol{U}}_2 = \vec{\boldsymbol{U}}$.

The momentum equation of the model based on interface tracking method in a certain direction, e.g., x-direction, is shown as

$$\rho \frac{\partial U}{\partial t} + \rho \nabla \cdot (U \vec{\boldsymbol{U}}) = -\frac{\partial p}{\partial x} + \nabla \cdot (\mu \underline{D}_x) + M_x + \rho g_x \tag{7}$$

where U stands for the x-direction component of the velocity. Introducing the geometric conservation equation of $\alpha_1 + \alpha_2 = 1$, and the expressions of the volume fraction weighted averaged density and dynamic viscosity, $\rho = \sum \alpha_k \rho_k$ and $\mu = \sum \alpha_k \mu_k$, which are also used in the model based on interface tracking method, Eq. (7) can be rearranged as

$$\sum_{k=1}^{2} \left[\alpha_k \rho_k \frac{\partial U}{\partial t} + \alpha_k \rho_k \nabla \cdot (U \vec{\boldsymbol{U}}) \right] = \sum_{k=1}^{2} \left[-\alpha_k \frac{\partial p}{\partial x} + \nabla \cdot (\alpha_k \mu_k \vec{\underline{\boldsymbol{D}}}_x) + \alpha_k \rho_k g_x \right] + M_x \tag{8}$$

Similar to the continuity equation, the above equation can also be split into two equations as follows:

$$\alpha_k \rho_k \frac{\partial U}{\partial t} + \alpha_k \rho_k \nabla \cdot (U \vec{\boldsymbol{U}}) = -\alpha_k \frac{\partial p}{\partial x} + \nabla \cdot (\alpha_k \mu_k \vec{\underline{\boldsymbol{D}}}_x) + \alpha_k \rho_k g_x + M_{xk} \tag{9}$$

where the notation k means the phase k, with the value of 1 or 2 and $M_x = \sum M_{xk}$. It is obvious that Eq. (9) is the form of the momentum equation in the two-fluid model, thought in the non-conservative form.

Based on the above derivations, the controlling equations of the model based on interface tracking method can be written in the following form:

$$\begin{aligned} &\frac{\partial}{\partial t}(\alpha_k \rho_k) + \nabla \cdot (\alpha_k \rho_k \vec{\boldsymbol{U}}_k) = 0 \\ &\alpha_k \rho_k \frac{\partial \vec{\boldsymbol{U}}_k}{\partial t} + \alpha_k \rho_k \nabla \cdot (\vec{\boldsymbol{U}}_k \vec{\boldsymbol{U}}_k) = -\alpha_k \nabla p + \nabla \cdot (\alpha_k \mu_k \vec{\underline{\boldsymbol{D}}}_k) + \vec{\boldsymbol{M}}_k + \alpha_k \rho_k \vec{\boldsymbol{g}} \end{aligned} \tag{10}$$

Obviously, the same form as the two-fluid model has been attained.

In the two-fluid model, the governing equations consist of the continuity equation and the momentum equations of individual phase. However, the governing equations only consists of one set of continuity equation and momentum equations in the model based on interface tracking method, where the two phases are considered as one phase, which means that the two phases share the same velocity field. According to the above derivations, the continuity equations and the momentum equations for one phase can be rearranged as the corresponding equations for two phases with a special case of $\vec{\boldsymbol{U}}_k = \vec{\boldsymbol{U}}$. It is also shown that the governing equations of the model based on interface tracking method are a subset of those of the two-fluid model. The two models are equivalent to each other in the case of $\vec{\boldsymbol{U}}_k = \vec{\boldsymbol{U}}$, which makes it available to write the governing equations as a unified form for the coupled model. As such, it is convenient to construct the solution strategy for the new model.

4.2. The solution strategy and the unified solution framework

The coupling of the two basic models is a direct way to keep the advantages of the two models. However, building a unified form of

the governing equations and a unified solution framework, which are shared by the two models, is necessary. Meanwhile, dealing with the special grids containing both the LSI phase and the SSI phase is also important.

The form of the governing equations of the model based on interface tracking method is a particular form of the two-fluid model when the two phases share the same velocity field. Obviously, the equations for the two models can be solved by the solution strategy for general two-fluid model, if the governing equations for the model based on interface tracking method are written in the form the same as the two-fluid model and each phase is regarded as a continuous phase occupying the whole domain as in the two-fluid model. However, in the coupled model, the governing equations of three phases are concerned. The detailed solution strategy is covered later.

The MCBA–SIMPLE algorithm is adopted as the basic strategy when solving with the two-fluid model. As mentioned above, in this algorithm, the pressure-correction equations are derived not by continuity equation of single phase but by the sum of continuity equations of all phases. This algorithm includes two characteristics. One is that this algorithm can easily extend the usual manipulations for two phases to more phases and the other is that many techniques developed for single phase can be applied to multiphase flow. These characteristics can be embedded into the new model in the process of coupling. This coupling inherits the characteristics of the MCBA–SIMPLE algorithm and makes the new model capable of dealing with more complex situations such as more than three phases or groups. All derivations and manipulations as follows proceed in the framework of this algorithm.

For the grids occupied by the three phases, special treatments are necessary. For the grids occupied by liquid phase, the solution is gained only by the algorithm for single phase, and for the grids occupied by two phases, e.g., liquid phase and LSI or SSI phase, the model based on interface tracking method or the two-fluid model is available. However, the coexistence of three phases in one grid results in more complexities. In the coupled model, a manipulation called "volume fraction redistribution" is performed for the special case. The manipulation is carried out by three steps. Firstly, transform the real values of the volume fractions of two phases, e.g., phase 1 and phase 2, so that this grid is occupied by only the two phases. Secondly, based on the resultant volume fractions of step 1, the related calculations and derivations of physical variables for solving Navier–Stokes equations for the two phases are performed. Finally, perform the inverse calculations for volume fractions so that the volume fractions of the two phases come back to the real ones. Simultaneously, the physical variables, e.g., the forces or the momentum exchange terms in momentum equations calculated in step 2 should also be changed proportionally. The manipulation of "volume fraction redistribution" will be extremely critical for the proposed model, and the detailed procedures of the implementation will be presented to in the next subsections.

4.3. The governing equations

In the coupled model, all fluids are divided into three phases: the liquid phase, the LSI phase and the SSI phase. The volume fraction of each phase is denoted by α. The subscript of α refers to one of these phases (1 for liquid phase, 2 for LSI phase and 3 for SSI phase) as shown in Fig. 1b.

As mentioned above, in the unified framework of solution strategy, the governing equations of each phase are written in the same form as those of the two-fluid model, shown as Eq. (10). Here the phase change is of no consideration.

For the governing equations in new form, solving the momentum equations of phase 1 and phase 2 should achieve the same velocity field, because the large-length-scale interfaces are formed by phase 1 and phase 2. However, for the governing equations of usual two-fluid model, the two phases have different velocity fields. This is the essential difference between the new governing equations and those of the usual two-fluid model, though they look like each other.

4.4. The pressure-correction equations

The following derivations are all for the case in which grids are occupied by three phases. In this process, the special treatment called "volume fraction redistribution" mentioned above is implemented for all grids. Thus, the conclusions are obtained for general case. The cases in which grids are occupied by one or two phases can be achieved easily.

Considering the incompressibility of fluids, the continuity equations of each phase are given by

$$\frac{\partial \alpha_k}{\partial t} + \nabla \cdot (\alpha_k \vec{\boldsymbol{U}}_k) = 0 \tag{11}$$

To implement the manipulation of "volume fraction redistribution", the volume fractions of phase 1 and phase 3, α_1 and α_3, are selected for transformation. This selection is due to two considerations. One is that the advection of the large-length-scale interfaces is calculated with the methods different from those of small-scale interfaces. The other is that there are direct interactions between the liquid phase and the SSI phase.

In the first step of the manipulation, the transformed volume fractions of the two phases occupy the whole grid, which means that the sum of the two transformed volume fractions should be 1. If the transformed value Φ is denoted by Φ', then $\alpha'_1 + \alpha'_3 = 1$. In view of the physical interactions between the two phases, the relative ratio of the volume fractions of the two phases should be maintained. Obviously, the transformation relationships of $\alpha'_1 = \alpha_1/(1-\alpha_2)$ and $\alpha'_3 = \alpha_3/(1-\alpha_2)$ satisfy the above two requirements.

The continuity equations of three phases can be modified as

$$\begin{aligned} &\frac{\partial \alpha'_1}{\partial t} + \nabla \cdot (\alpha'_1 \vec{\boldsymbol{U}}_1) = 0 \\ &\frac{\partial \alpha_2}{\partial t} + \nabla \cdot (\alpha_2 \vec{\boldsymbol{U}}_2) = 0 \\ &\frac{\partial \alpha'_3}{\partial t} + \nabla \cdot (\alpha'_3 \vec{\boldsymbol{U}}_3) = 0 \end{aligned} \tag{12}$$

Based on the transformed volume fractions, adding the continuity equations of phase 1 and phase 3 gives

$$\nabla \cdot (\alpha'_1 \vec{\boldsymbol{U}}_1 + \alpha'_3 \vec{\boldsymbol{U}}_3) = 0 \tag{13}$$

where the identical equation $\alpha'_1 + \alpha'_3 = 1$ is used.

In the manipulation, the inverse transformation to the original condition is necessary. Under the original condition, the phase 1 and phase 3 only occupy the portion $(1-\alpha_2)$ of the whole grid volume. If the two phases are regarded as a whole, the contribution of the volume occupancy of the two phases is calculated by multiplying Eq. (13) with $(1-\alpha_2)$. Then the continuity equations of all phases are added to yield the overall volume conservation equation, that is

$$\frac{\partial \alpha_2}{\partial t} + \nabla \cdot (\alpha_2 \vec{\boldsymbol{U}}_2) + (1-\alpha_2)\nabla \cdot (\alpha'_1 \vec{\boldsymbol{U}}_1 + \alpha'_3 \vec{\boldsymbol{U}}_3) = 0 \tag{14}$$

The overall volume conservation equation will be employed to derive the pressure-correction equations, which is also implemented in the MCBA–SIMPLE algorithm.

It should be noted that, in the proposed model, α_2 is used to indicate the accurate location of large-length-scale interface, although its physical meaning is volume fraction. Thus, special

interface tracking algorithms, such as VOF method and Level Set method, should be employed. By denoting the velocity field of interface advection as $\vec{U}_2$, the equation used to advect the interface denoted by α_2 is given by

$$\frac{\partial \alpha_2}{\partial t} + \vec{U}_2 \cdot \nabla \alpha_2 = 0 \tag{15}$$

Subtracting the above equation from the continuity equation of phase 2 gives $\nabla \cdot \vec{U}_2 = 0$, which corresponds to the incompressibility of phase 2 fluid. Subtracting Eq. (15) from the new overall volume conservation equation yields

$$\alpha_2 \nabla \cdot \vec{U}_2 + (1-\alpha_2)\nabla \cdot (\alpha_1' \vec{U}_1 + \alpha_3' \vec{U}_3) = 0 \tag{16}$$

which is the equation that can be shared by the two basic models. Assigning $\alpha_2 = 0$ or 1 corresponds to one of the two basic models, respectively. When α_2 is equal to 1, the above equation is reduced to $\nabla \cdot \vec{U}_2 = 0$, which is used in the model based on interface tracking method. If α_2 is equal to 0, then $\nabla \cdot (\alpha_1' \vec{U}_1 + \alpha_3' \vec{U}_3) = 0$, which is used for the two-fluid model. However, for the special grid where all three phases are present, the volume conservation for the phase 2 and the other two phases are usually not guaranteed in the process of numerical calculation. The reason is that only one pressure field is used in the proposed model and that two different pressure fields are employed in the two basic models. Considering the importance of the movement of large-length-scale interface and for the sake of simplicity, the volume conservation of phase 2 is guaranteed preferentially. If the large-length-scale interface is present in the grid, $\nabla \cdot \vec{U}_2 = 0$ is chosen to solve. This choice can cause error in the zones near interface. However, this choice has less influence on the other zones. Therefore, the modified overall volume conservation equation is given by

$$\begin{cases} \nabla \cdot \vec{U}_2 = 0, \text{when phase 2 is present in the grid} \\ \nabla \cdot (\alpha_1' \vec{U}_1 + \alpha_3' \vec{U}_3) = 0, \text{ when phase 2 is absent in the grid} \end{cases} \tag{17}$$

which is the final overall volume conservation equation employed to derive the pressure-correction equation in the proposed model within the solution framework of MCBA–SIMPLE algorithm.

The procedure of forming the pressure-correction equation is the same as that in Appendix A, where the pressure correction field is related to the velocity correction field. In the process of deriving the pressure-correction equation, the critical work to do is to substitute the relationships of the pressure correction field and the velocity correction field for individual phase into the final overall volume conservation equation. Through this substitution, the final overall volume conservation equation can be rearranged as

$$\begin{cases} \nabla \cdot [(\alpha_1 + \alpha_2) D_2 \nabla p'] = \nabla \cdot \vec{U}_2^*, \text{when phase 2 is present in the grid} \\ \nabla \cdot [(\alpha_1' \alpha_1 D_2 + \alpha_3' \alpha_3 D_3) \nabla p'] \\ = \nabla \cdot (\alpha_1' \vec{U}_1^* + \alpha_3' \vec{U}_3^*), \text{when phase 2 is absent in the grid} \end{cases} \tag{18}$$

where the momentum equations shared by phase 1 and phase 3 are used, which will be covered later. The notations have been denoted in Appendix A. After solving Eq. (18), new pressure field and velocity field can be obtained by Eq. (A.10) of Appendix A.

In this section, the modified continuity equations are employed in the process of deriving the pressure-correction equation, which results from the manipulation of "volume fraction redistribution". In the manipulation, the particularity of phase 2 has been taken into account. Another merit of the derivation is that the derivative of α_2 is not included, which ensures the numerical stability of calculation.

4.5. The momentum equations

In the general two-fluid model, the velocity fields of each phase are obtained by solving the momentum equations of the corresponding phase. However, the presence of large scale interface in a grid makes special treatment required before solving momentum equations in the coupled model.

In the proposed model, one important characteristic of the model based on interface tracking method, that is, the two phases (phase 1 and phase 2) composing large-length-scale interface share the same velocity field, is embodied in the MCBA–SIMPLE algorithm. Thus, it is available to solve one set of momentum equations for the two phases.

Considering the principle of the equivalence of the two forms when sharing the same velocity field, the shared momentum equations for phase 1 and phase 2 can be obtained. The shared velocity field is denoted by $\vec{U}_m$, i.e., $\vec{U}_1 = \vec{U}_2 = \vec{U}_m$. The momentum equations of the two phases can be written as

$$\begin{aligned} \alpha_1 \rho_1 \frac{\partial \vec{U}_m}{\partial t} + \alpha_1 \rho_1 \nabla \cdot (\vec{U}_m \vec{U}_m) &= -\alpha_1 \nabla p + \nabla \cdot (\alpha_1 \mu_1 \vec{D}_1) + \vec{M}_1 + \alpha_1 \rho_1 \vec{g} \\ \alpha_2 \rho_2 \frac{\partial \vec{U}_m}{\partial t} + \alpha_2 \rho_2 \nabla \cdot (\vec{U}_m \vec{U}_m) &= -\alpha_2 \nabla p + \nabla \cdot (\alpha_2 \mu_2 \vec{D}_2) + \vec{M}_2 + \alpha_2 \rho_2 \vec{g} \end{aligned} \tag{19}$$

Adding the two equations gives

$$\begin{aligned} \rho_m \frac{\partial \vec{U}_m}{\partial t} + \rho_m \nabla \cdot (\vec{U}_m \vec{U}_m) = &-(\alpha_1 + \alpha_2)\nabla p + \nabla \cdot (\mu_m \vec{D}_m) \\ &+ \vec{M}_m + \rho_m \vec{g} \end{aligned} \tag{20}$$

where $\rho_m = \alpha_1 \rho_1 + \alpha_2 \rho_2$ and $\mu_m = \alpha_1 \mu_1 + \alpha_2 \mu_2$ are used. It is noted that ρ_m is the summation of the macroscopic densities of the two phases, not the macroscopic densities of all three phases. The two macroscopic densities are equal when the phase 3 is absent. Similarly the expression $(\alpha_1 + \alpha_2)$ is equal to $(1 - \alpha_3)$ and is equal to 1 only when the phase 3 is absent.

Eq. (20) is used to solve the velocity field shared by phase 1 and phase 2. The velocity fields of phase 3 are obtained by solving its original momentum equations shown as

$$\alpha_3 \rho_3 \frac{\partial \vec{U}_3}{\partial t} + \alpha_3 \rho_3 \nabla \cdot (\vec{U}_3 \vec{U}_3) = -\alpha_3 \nabla p + \nabla \cdot (\alpha_3 \mu_3 \vec{D}_3) + \vec{M}_3 + \alpha_3 \rho_3 \vec{g} \tag{21}$$

When all three phases are present in a grid, special treatments for the shared momentum exchange term $\vec{M}_m$ are needed.

The physical meaning of $\vec{M}_m$ is the external forces acting on the fluid of phase 1 and phase 2 per unit volume. Based on the practical situations of gas–liquid two-phase flow, $\vec{M}_m$ includes two parts: the force induced by the interface between phase 1 and phase 2 per unit volume, e.g., surface tension force and the interactive force between phase 1 and phase 3 per unit volume, e.g., the drag force, the lift force, the wall force, etc. The two parts of $\vec{M}_m$ are defined as $\vec{M}_{m,L}$ and $\vec{M}_{m,S}$, respectively. The manipulation of "volume fraction redistribution" is implemented when calculating $\vec{M}_m$.

For the sake of simplicity, the surface tension force is taken as an example of $\vec{M}_{m,L}$. Here the surface tension force acts only on phase 1 and phase 2. When the phase 3 is present, the effect of surface tension force should be reduced in proportion to $(1 - \alpha_3)$. If $\vec{M}'_{m,L}$ denotes the force induced by interface per unit volume when only phase 1 and phase 2 are present, then the relationship $\vec{M}_{m,L} = (1 - \alpha_3) \cdot \vec{M}'_{m,L}$ is obtained. $\vec{M}_{m,L}$ can be calculated in three steps. The first step is to modify the volume fractions of phase 1 and phase 2, assuming that only the two phases are present. The second step is to calculate $\vec{M}'_{m,L}$. Finally $\vec{M}_{m,L}$ is obtained using

the relationship $\vec{M}_{m,L} = (1-\alpha_3)\cdot\vec{M}'_{m,L}$. The essence of these three steps is to implement "volume fraction redistribution". The process of calculating $\vec{M}_{m,L}$ is shown in Fig. 3a.

The calculation of $\vec{M}_{m,S}$ is very similar to that of $\vec{M}_{m,L}$. Based on physics, $\vec{M}_{m,S}$ acts only on phase 1 and phase 3. Thus, $\vec{M}_{m,S}$ is proportional to the sum of the volume fractions of the two phases. If $\vec{M}'_{m,S}$ is considered as the force between phase 1 and phase 3 per unit volume when only phase 1 and phase 3 are present, the relationship $\vec{M}_{m,S} = (1-\alpha_2)\cdot\vec{M}'_{m,S}$ is given. The manipulation of "volume fraction redistribution" is implemented to calculate $\vec{M}_{m,L}$. Firstly, modify the volume fractions of phase 1 and phase 2, assuming that only the two phases are present. Then $\vec{M}'_{m,S}$ is obtained with the modified volume fractions. Finally $\vec{M}_{m,S}$ is given by the relationship $\vec{M}_{m,S} = (1-\alpha_2)\cdot\vec{M}'_{m,S}$. The process of calculating $\vec{M}_{m,S}$ is shown in Fig. 3b.

4.6. The volume fraction of each phase

In the MCBA–SIMPLE algorithm with n phases, $(n-1)$ continuity equations are employed to calculate the volume fraction fields of the corresponding phases, and the volume fraction field of the remaining phase is obtained using the geometric conservation equation $\sum \alpha_i = 1$. For these continuity equations, they are considered as common partial differential equations and are solved using the common method, i.e., the partial differential equation is discretized into the set of linear equations and solved. The common method is also the solution method of momentum equations and pressure correction equations. However, in the proposed model, the presence of large-length-scale interfaces requires the interfaces to be sharp between phase 1 and phase 2. The common solution for partial differential equations produces serious numerical diffusion in the grids near interface, resulting in the incapability of making sharp interface and accurately locating interface. Thus, a special method for the continuity equation indicating interface should be suggested to evaluate the interfaces between phase 1 and phase 2.

Without losing generality, the volume fraction of phase 2, α_2, is selected to indicate the interface. In the proposed model, α_2 should meet two points. One is that its value should represent the volume fraction occupied by the fluid of phase 2 in a grid. The other is that it should have as less numerical diffusion as possible. In the interface tracking methods reported, only the VOF method can satisfy the two requirements. In the VOF method, the interface tracking is based on the color function, which marks the fluids in the following way (Puckett et al., 1997)

$$f = \begin{cases} 0, & \text{if place is occupied by the fluid of phase 1} \\ 1, & \text{if place is occupied by the fluid of phase 2} \end{cases}$$

The color function f is evaluated in a discrete grid as a volume average

$$\alpha = \frac{1}{V_{\text{grid}}}\int_{V_{\text{grid}}} f\cdot dV$$

where V_{grid} is the volume of grid. The interface advection equation, Eq. (15), is obtained when integrating Eq. (2) over the whole domain in the grid. It can advect explicitly the volume fraction of phase 2, α_2. A similar result can be obtained when $k = 1$. The VOF method includes the interface reconstruction and an advection algorithm. There are several algorithms with different accuracies and complexities to do this work. Here we employ the VOF/PLIC method. The concrete description of the VOF/PLIC method can be found in Gueyffier et al. (1999).

For the stability of calculation, the volume fraction field of phase 1 is calculated using the geometric conservation equation, after obtaining the volume fraction fields of phase 2 and 3.

4.7. The solution procedure

The solution procedure of the proposed model is to follow the framework of MCBA–SIMPLE. With the supplementary specifications mentioned in the previous subsections, the proposed model

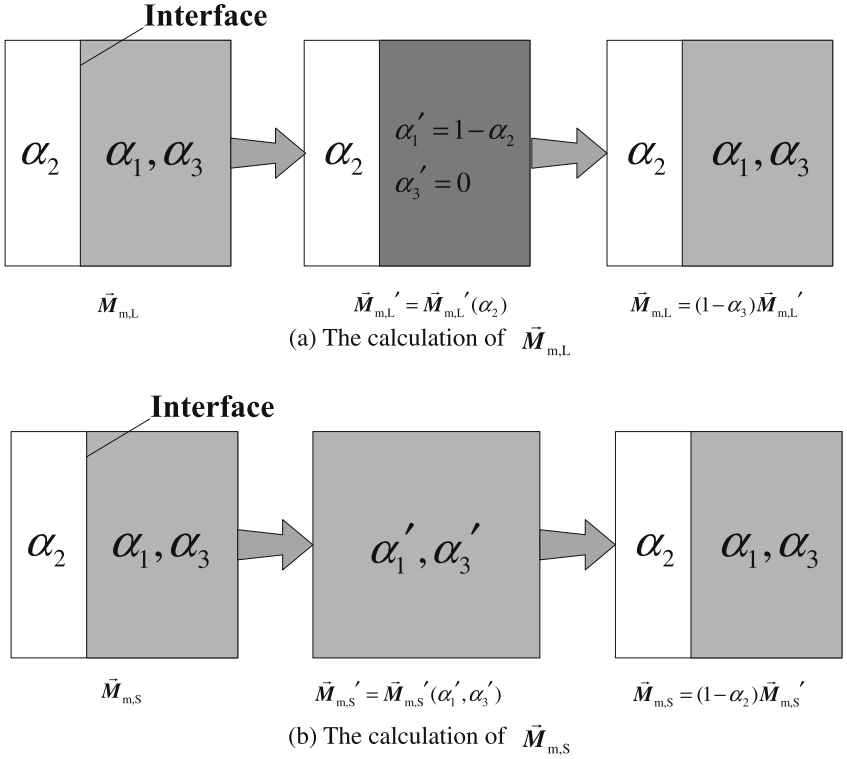

Fig. 3. The calculation of $\vec{M}_m$, including $\vec{M}_{m,L}$ and $\vec{M}_{m,S}$.

can be solved in the modified solution procedure of MCBA–SIMPLE as follows:

(1) Solve Eq. (20) for the velocity field shared by phase 1 and phase 2 and solve the momentum equations of Eq. (21) for the velocity field of phase 3.
(2) Solve the pressure-correction equation, Eq. (18). The equation is a comprehensive result of global mass conservation and the special treatment for the proposed model.
(3) Correct velocities and pressure with Eq. (A.10).
(4) Solve Eq. (11) with $k = 3$ for the volume fraction field of phase 3. The volume fraction field of phase 2 is obtained by Eq. (15) with the VOF/PLIC method, and the volume fraction field of phase 1 is obtained by the geometric conservation equation $\sum \alpha_i = 1$.
(5) Solve other scalar equations.
(6) Return to the first step and repeat until convergence.
(7) Go to the next time step and repeat the above 6 steps.

4.8. The volume addition of LSI phase due to the coalescence

The interactions between LSI phase (phase 2) and SSI phase (phase 3) include two forms, the breakup from LSI phase to SSI phase and the coalescence when SSI phase comes into LSI phase. However, because of the limited knowledge of breakup, this subsection only focuses on coalescence.

As mentioned above, Eq. (15) is employed to advect the large-length-scale interface and α_2 is used to indicate the location of the interface. The movement of the interface is determined by $\vec{\boldsymbol{U}}_2$ ($\vec{\boldsymbol{U}}_m$). In the process of coalescence, the volume of LSI phase can grow up because some portion of SSI phase comes into LSI phase. Thus, the effect of volume addition can be formulated by modifying the original value of $\vec{\boldsymbol{U}}_m$. Then the relationship $\vec{\boldsymbol{U}}'_m = \vec{\boldsymbol{U}}_m + \vec{\boldsymbol{U}}_{\mathrm{Add}}$ is built, where $\vec{\boldsymbol{U}}'_m$ denotes the modified field of $\vec{\boldsymbol{U}}_m$ and $\vec{\boldsymbol{U}}_{\mathrm{Add}}$ is the additional velocity field due to the SSI phase flowing into the LSI phase.

In the VOF/PLIC method, the operator split advection algorithm is used, in which one calculation step is performed for one spatial direction. Likewise, it is appropriate to illustrate the expression of $\vec{\boldsymbol{U}}_{\mathrm{Add}}$ in only one direction. Take the x-direction as an example, as shown in Fig. 4. U_m and U_3 represent the interface velocity and the velocity of phase SSI phase near the interface, respectively. Δt is the fractional time step. It is assumed that the velocities mentioned above are kept constant in the time step Δt and that the cross-sectional area is set as 1. Without losing generality, at the initial time the interface is on the left edge of the grid. In the time step, the volume of phase 1 flowing into the grid is $U_m \Delta t$. If the velocity of phase 3, U_3, is greater than U_m, the fluid of phase 3 can catch up with the interface and come into the fluid of phase 2. Then the volume of phase 3 flowing to phase 2 is calculated as $\alpha_3(U_3 - U_m)\Delta t$ in the time step, which is the addition of the volume of phase 2 in the grid. Then the volume of phase 1 in the grid becomes $[U_m \Delta t - \alpha_3(U_3 - U_m)\Delta t]$. After rearranging, the corresponding modified velocity of the interface is $[U_m - \alpha_3(U_3 - U_m)]$. Then the expression of the additional velocity is $[-\alpha_3(U_3 - U_m)]$. The similar results can be achieved in other two directions.

Considering all the conditions when some portion of SSI phase can come into LSI phase, the following expression of the additional velocity, $\vec{U}_{\mathrm{Add}}$, is given by

$$\vec{\boldsymbol{U}}_{\mathrm{Add},s} = \begin{cases} -\alpha_3 \max[(\vec{\boldsymbol{U}}_3 - \vec{\boldsymbol{U}}_m)_s, 0], & \text{if} \quad \frac{\partial \alpha_2}{\partial s} > 0 \\ -\alpha_3 \min[(\vec{\boldsymbol{U}}_3 - \vec{\boldsymbol{U}}_m)_s, 0], & \text{if} \quad \frac{\partial \alpha_2}{\partial s} < 0 \end{cases} \tag{22}$$

where s stands for x-, y- or z-direction, the three directions in space, respectively. $\vec{\boldsymbol{U}}_{\mathrm{Add},s}$ corresponds to the component of $\vec{\boldsymbol{U}}_{\mathrm{Add}}$ in one of the three directions.

5. Results and discussion

The performance of the proposed model is assessed in this section by applying it to four gas–liquid two-phase flow problems. The first problem is to simulate the movement and deformation of a single gas bubble in liquid with various dimensionless numbers. The second problem deals with the upward laminar dilute bubbly flow in a vertical pipe. The two problems are aimed at the two extreme cases of the proposed model, the case of equivalence to the model based on interface tracking method and that of only using the two-fluid model. In the third problem a rising large gas bubble is followed by bubbly flow in a vertical pipe. Reversely, in the last problem bubbly flow is followed by a rising large gas bubble, where the volume change of the large bubble since some small bubbles coming into the large bubble must be taken into account.

5.1. The movement and deformation of a single gas bubble in stagnant viscous liquid

In this problem, the movement and deformation of a single gas bubble in stagnant viscous liquid are simulated. The simulations are performed with several groups of dimensionless numbers, which represents the relative dominance of various physical properties. The calculated results are compared with previous experimental results and the bubble diagram of Grace (1973).

The typical model used to solve the problem is based on interface tracking method, such as VOF or Level set, because attention is paid to the shape of bubble. Thus, the length scale of the interface should be much larger than that of grid. For the proposed model, the absence of SSI phase is absent in this problem. When the volume fraction of phase 3 is specified as 0, the corresponding redistributed volume fraction, α'_3, should also be 0, which means that

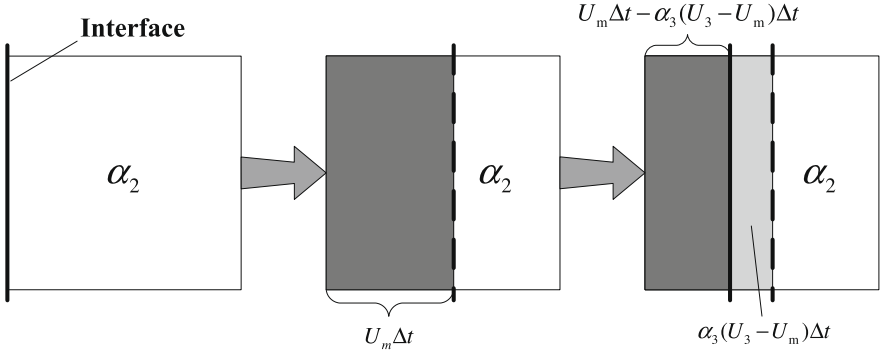

Fig. 4. The advection of large-length-scale interface when some portion of SSI phase flows into LSI phase.

$\alpha_1' = 1$. Finally Eq. (17), the overall volume conservation equation, is reduced to

$$\nabla \cdot \vec{\boldsymbol{U}}_m = 0$$

which is the same as the continuity equation in the model based on interface tracking method. Meanwhile, the momentum equations shared by phase 1 and phase 2 are equivalent to those in the model based on interface tracking method, which have been obtained with the derivation process in Section 4.1. The equivalence ensures that all the governing equations for the proposed model are the same as those for the model based on interface tracking method, which will result in the same results. Surface tension effects are calculated with the continuum surface force (CSF) model of Brackbill et al. (1992) and act in the form of source term in momentum equations. The solution strategy is still MCBA–SIMPLE algorithm, which is reduced to the solution used to solve the model based on interface tracking method in this problem.

A two-dimensional cylindrical coordinate assuming axial symmetry about a straight line in the gravitational direction is employed. A uniform rectangular grid system with the grid size of 0.001 m is used, which is enough to ensure results to be independent of grid for this problem. The computational domain of 0.08 m × 0.15 m (0.08 m in radial direction and 0.15 m in axial direction) is employed. The time step is set as 10^{-4} s. The single bubble ascends in the stagnant viscous liquid and finally its shape and its terminal rise velocity will not change. The total time is set as 0.3 s, which is long enough to stabilify the movement of the bubble. At initial time the shape of the bubble is assumed to be a sphere of a certain diameter, whose center is on the symmetrical axis. The value of the diameter is determined by the volume of bubble.

In the following comparisons, the dimensionless numbers of Morton (Mo), Eotvos (Eo) and Reynolds (Re) are used, which are given by

$$Mo = \frac{g\mu_1^4\Delta\rho}{\rho_1^2\sigma^3}$$

$$Eo = \frac{g\Delta\rho d_e^2}{\sigma}$$

$$Re = \frac{\rho_1 v_\infty d_e}{\mu_1}$$

where the effective diameter d_e is defined as the diameter of a spherical bubble with the same volume as the bubble under consideration. In this problem, the effective diameter is equal to the diameter of bubble at initial time. In the Reynolds number v_∞ represents the terminal rise velocity of the bubble.

Previous experimental results are employed for comparisons with the calculated results. Fig. 5 shows the comparisons for three cases: (a) $Eo = 116$, $Mo = 5.5$ presented by Bhaga and Weber (1981); (b) $Eo = 39$, $Mo = 6.5 \times 10^{-2}$ presented by Hnat and Buckmaster (1976); and (c) $Eo = 73$, $Mo = 6.5 \times 10^{-2}$ by Hnat and Buckmaster (1976). The calculated shapes and velocity fields are shown on the right side and the experimental results on the left side. As shown in Fig. 5, the calculated bubble shapes agree well with previous experimental results. The calculated Re values are close to the values of previous studies. In Fig. 5, the different display densities of velocity vectors are due to the different bubble volumes in the three cases. More accurate results have been shown by Ohta et al. (2005), because the adaptive mesh refinement (AMR) (Sussman et al., 1999) and the more accurate calculation of surface tension have been applied. Nevertheless, the calculated results are enough to demonstrate the equivalence of the proposed model to the model based on interface tracking method.

Table 1
Three groups of Morton and Eotvos numbers for simulations of bubbles in different regimes according to the bubble diagram of Grace.

Case	Mo	Eo	Re_G	Re_C	Bubble regime
A	0.001	1.0	1.7	1.6	Spherical
B	0.1	10.0	4.6	4.3	Ellipsoidal
C	1000	100.0	1.5	1.6	Dimpled/ellipsoidal

According to Grace (1973), the shapes and rise velocities of bubbles in stagnant viscous liquids can be condensed into one diagram, provided that an appropriate set of dimensionless numbers is used. In this diagram, three groups of Morton and Eotvos numbers are selected for the simulations of the bubbles in different regimes according to the bubble diagram of Grace, as listed in Table 1. In this table Re_G and Re_C represent the bubble Reynolds number obtained from the bubble diagram and the computed ones, respectively.

In the simulation, the diameter of the sphere at initial time is set as 0.012 m. A fixed density and viscosity ratio of 1000 is used. The density/viscosity of phase 1 equals 1000 times the density/viscosity of phase 2, where the density of phase 1 is set as 1000 kg/m^3 and the density of phase 2 as 1 kg/m^3. The ratio is believed to mimic gas–liquid system with high density and viscosity ratio. Other physical parameters are determined by the dimensionless numbers.

Fig. 6 shows the computed shapes of bubbles for the three groups of Morton and Eotvos numbers, where the dash dotted line represents the symmetric axis. It can be seen that the computed Reynolds numbers and the bubble shapes are in good agreements with the experimental data from the bubble diagram of Grace.

5.2. Fully developed upward laminar dilute bubbly flow in a vertical pipe

The problem involves the prediction of radial phase distribution in upward laminar air-oil flow in a vertical pipe. There are some experimental and numerical studies on the bubbly flow under laminar condition. Song et al. (2001) has studied the phase distributions for upward laminar dilute bubbly flows with non-uniform

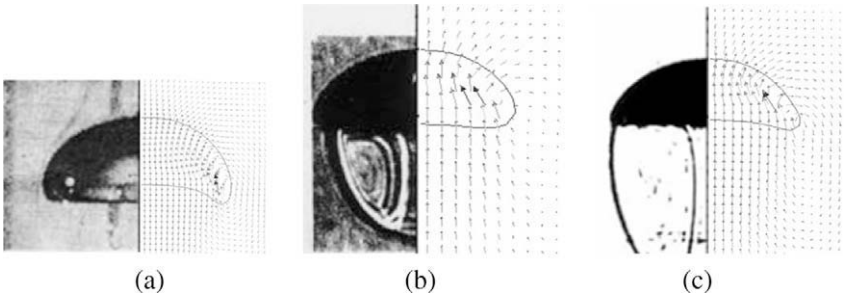

Fig. 5. Comparisons of the calculated results with experimental results.

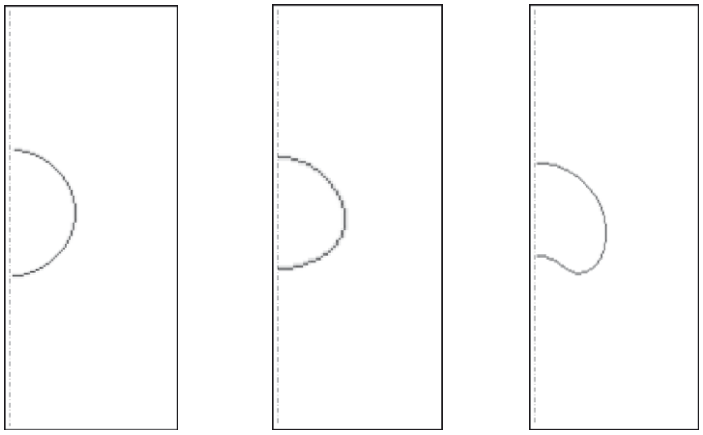

Fig. 6. Computed bubble shapes for the different bubble regimes.

bubble sizes in a vertical pipe. This problem, in which some experimental data of Song is used, is chosen to show an extreme case as well, where the proposed model is equivalent to the two-fluid model.

In general, the two-fluid model is employed for the dispersed flow such as gas–liquid bubbly flow. In this flow pattern, the bubble swarm consisting of many small bubbles moves in a channel or a duct. The length scales of the interfaces of these small bubbles are so small that only the averaged values of physical parameters, such as volume fraction, pressure, velocity of single phase and so on are concerned and the movement and deformation of individual interface is ignored. The length scales of the interfaces usually have the same order as or smaller than those of calculating grids.

The large-length-scale interface is absent in the problem, i.e., the volume fraction of phase 2 is specified as 0, which makes the proposed model equivalent to the two-fluid model. In this case, the momentum equations shared by phase 1 and phase 2, are degenerated to those only for phase 1. Meanwhile, Eq. (17) is reduced to

$$\nabla \cdot (\alpha_1' \vec{\boldsymbol{U}}_1 + \alpha_3' \vec{\boldsymbol{U}}_3) = 0$$

which is the standard form for the original MCBA–SIMPLE algorithm. Here the detailed solution procedures of the coupled model are implemented for solving the two-fluid model. In the solution procedures, the step of evaluating the large-length-scale interface defined by volume fraction of phase 2 is ignored.

Compared to the momentum equation deduced with the ensemble averaging method, the momentum exchange term of phase k can be written as (Drew and Passman, 1998)

$$\vec{\boldsymbol{M}}_k = \vec{\boldsymbol{M}}_{ki} - \tau_{ki} \cdot \nabla \alpha_k + (p_{ki} - p) \nabla \alpha_k$$

where the subscript i represents the interface, the term $\vec{\boldsymbol{M}}_{ki},\ \tau_{ki},\ p_{ki}$, represent the corresponding physical variable of phase k at the interface. Interfacial forces acting on each phase differ only in sign, hence

$$\vec{\boldsymbol{M}}_{1i} = -\vec{\boldsymbol{M}}_{3i}$$

For fully developed laminar bubbly flow in vertical pipe, the interfacial force term $\vec{\boldsymbol{M}}_{ki}$ is decomposed into several components:

$$\vec{\boldsymbol{M}}_{ki} = \vec{\boldsymbol{M}}_k^{\mathrm{Drag}} + \vec{\boldsymbol{M}}_k^{\mathrm{Lift}} + \vec{\boldsymbol{M}}_k^{\mathrm{Wall}}$$

The contribution of drag force to $\vec{M}_{ki},\ M_k^{\mathrm{Drag}}$ is given by Ishii and Zuber (1979)

$$\vec{\boldsymbol{M}}_1^{\mathrm{Drag}} = -\vec{\boldsymbol{M}}_3^{\mathrm{Drag}} = \frac{3}{8}\frac{C_D}{a}\alpha_3 \rho_1 |\vec{\boldsymbol{U}}_{\mathrm{r}}| \vec{\boldsymbol{U}}_r$$

where a is the bubble radius, $\vec{\boldsymbol{U}}_r = \vec{\boldsymbol{U}}_3 - \vec{\boldsymbol{U}}_1$ is the slip velocity and C_D is the drag coefficient. The drag coefficient could be modified to account for the bubble concentration effect (Ishii and Zuber, 1979). Then an appropriate drag coefficient is chosen as follows:

$$C_D = \frac{24(1 + 0.1Re^{0.75})}{Re}$$

where $Re = \frac{2\rho_1 |\vec{\boldsymbol{U}}_r| a}{\mu_1}$ is the particle Reynolds number.

The contribution of lift force, $\vec{\boldsymbol{M}}_k^{\mathrm{Lift}}$, is written in the following form (Drew and Lahey, 1979)

$$\vec{\boldsymbol{M}}_1^{\mathrm{Lift}} = -\vec{\boldsymbol{M}}_3^{\mathrm{Lift}} = C_L \alpha_3 \rho_1 \vec{\boldsymbol{U}}_r \times (\nabla \times \vec{\boldsymbol{U}}_1)$$

where C_L is the lift coefficient. Moraga et al. (1999) correlated the lift coefficient as a function of bubble Reynolds number and local shear Reynolds number. They also showed that C_L may be negative for large bubbles in high-shear flows. However, in this problem, C_L is chosen as 0.1, which was also recommended by Lopez de Bertodano (1992) for bubbly flows in vertical pipes.

The contribution of wall force, $\vec{\boldsymbol{M}}_k^{\mathrm{Wall}}$, arises from the fact that the relative velocity between bubble and wall is lower than that between bubble and the outer flow, which results in the pressure difference driving bubble away from the wall. It can be written as (Tomiyama et al., 1997)

$$\vec{\boldsymbol{M}}_1^{\mathrm{Wall}} = -\vec{\boldsymbol{M}}_3^{\mathrm{Wall}} = C_W \alpha_3 \rho_1 |\vec{\boldsymbol{n}}_z \cdot \vec{\boldsymbol{U}}_r|^2 \frac{4aRr}{(R^2 - r^2)^2} \vec{\boldsymbol{n}}_r$$

where R is the radius of pipe, $\vec{n}_z$ is the unit vector in the axial direction, $\vec{n}_r$ is the outward unit vector perpendicular to the wall and C_W is the wall coefficient. C_W is related to dimensionless numbers of We, Eo, Mo and Ca, which are used to describe the formation of bubble. In this problem, C_W is specified to be 0.08.

Lamb (1932) considered the potential flow around single sphere and the interfacial pressure difference is obtained

$$p_{1i} - p_1 = -C_p(1 - \alpha_3)\rho_1 |\vec{\boldsymbol{U}}_r|^2$$

where C_p is the pressure difference coefficient. In view of small gas density, the pressure difference induced by Bernoulli effect is negligible, i.e., $p_{2i} - p_2 = 0$. C_p was given by Xu (2004) as

$$C_p = \frac{1}{4} + \frac{16}{\sqrt{\pi Re^3}}$$

Table 2
Flow parameters for two experimental conditions.

Condition	a (mm)	Re	U_{SL} (m/s)	U_{SG} (m/s)
Condition 1	1.4	5.74	0.08	0.003
Condition 2	1.35	5.32	0.13	0.003

Considering the analysis of the forces acting on interfaces (Antal et al., 1991), the relationship $\tau_{1i} = \tau_{3i}$ is obtained. The additional stress, τ_1^{Re}, is added to the molecule viscous stress in presence of small bubbles. The expression of τ_1^{Re} was given by Nigmatulin (1979) and Sato et al. (1981).

$$\tau_1^{Re} = -\rho_1\alpha_3\left[\frac{3}{20}|\vec{\boldsymbol{U}}_r|^2 I + \frac{1}{20}\vec{\boldsymbol{U}}_r\vec{\boldsymbol{U}}_r\right] + 0.6\alpha_3 Re\mu_1(\nabla\vec{\boldsymbol{U}}_1 + \nabla\vec{\boldsymbol{U}}_1^T)$$

Two experimental conditions are selected for simulation using the above treatments. In the experiments, the working fluids are air and 25# transformer oil. The inner diameter of the pipe is 29 mm, while the densities of the working fluids are 1.2 kg/m^3 for air and 866 kg/m^3 for 25# transformer oil, respectively. The viscosity of the oil is 0.0316 Pa s. The working temperature is 20 °C. Other parameters of the two conditions are shown in Table 2.

The uniform grid system with the grid number of 29 in radial direction is employed, which is high enough to gain the grid independent results. Numerically predicted radial profiles of the void fraction (the volume fraction of phase 3) are presented in Fig. 7. The locations of the peaks and the distributions of the void fractions are in good agreements with the measurements. It has been shown that the gas is taken away from the pipe center due to the lift force, while the gas near wall is driven away to outer flow due to the wall force. Therefore the void fraction peak occurs in radial direction. Due to the lack of comprehensive knowledge of these coefficients in these empirical correlations, there are still differences in the distribution of local void fraction between numerical results and experimental data. Nevertheless, the characteristics of the proposed model have been demonstrated.

5.3. A rising large gas bubble followed by bubbly flow in a vertical pipe

In this problem, a rising gas bubble with large-length-scale interface followed by a swarm of small bubbles is simulated, including the interactions between them. In the second problem, only the interactions of the liquid phase and the SSI phase are simulated, whereas the LSI phase is of no consideration. However, in this subsection the LSI phase is taken into account. This problem is a typical example that can adequately show the advantages of the proposed model.

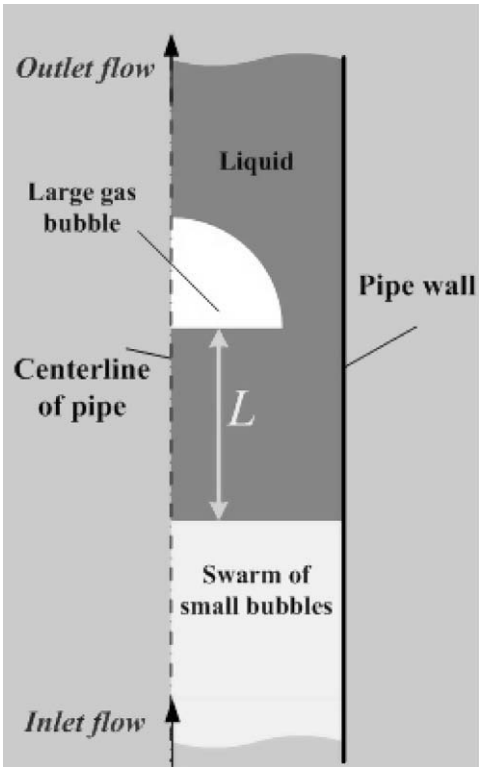

Fig. 8. The schematic diagram of computational domain at initial time in Section 5.3.

A two-dimensional coordinate system assuming axial symmetry about the centerline of the pipe is used. The radius of the pipe is 14 mm, and the pipe length is 150 mm. A uniform rectangular grid system of 14×150 is used. The schematic diagram of the problem at initial time and the computational domain is shown as Fig. 8. The initial shape of the large bubble is a hemisphere with a radius of 9 mm. The shape is simulated and finally a steady bubble shape is attained. The initial distance from the hemisphere bottom to the bottom of the computational domain, is 35 mm. Small bubbles of bubbly flow are injected into the pipe from the

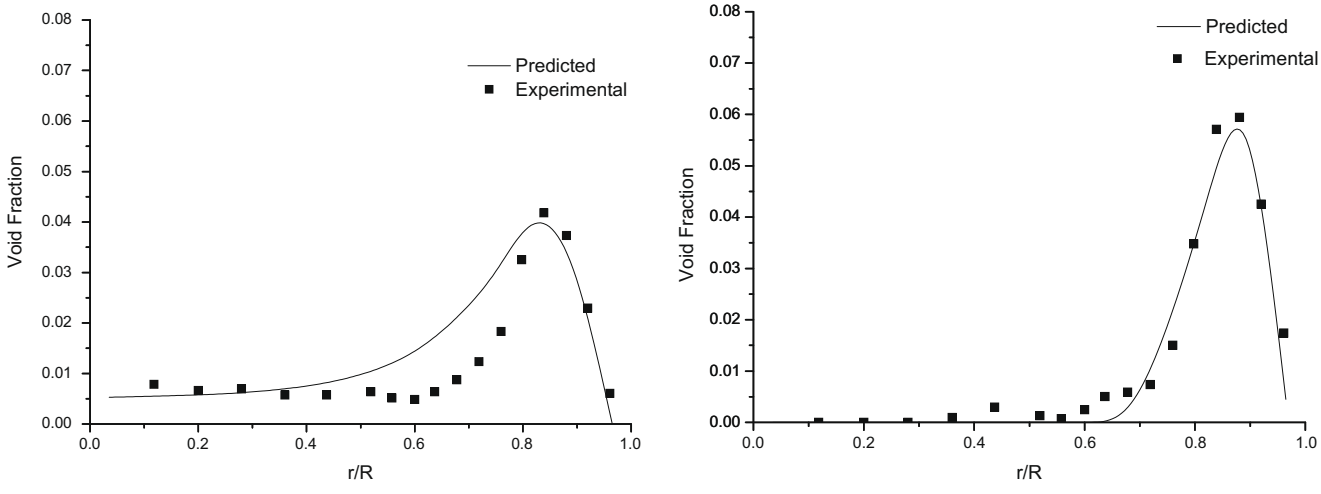

Fig. 7. Void fraction profiles for fully developed upward laminar bubbly flow in a vertical pipe.

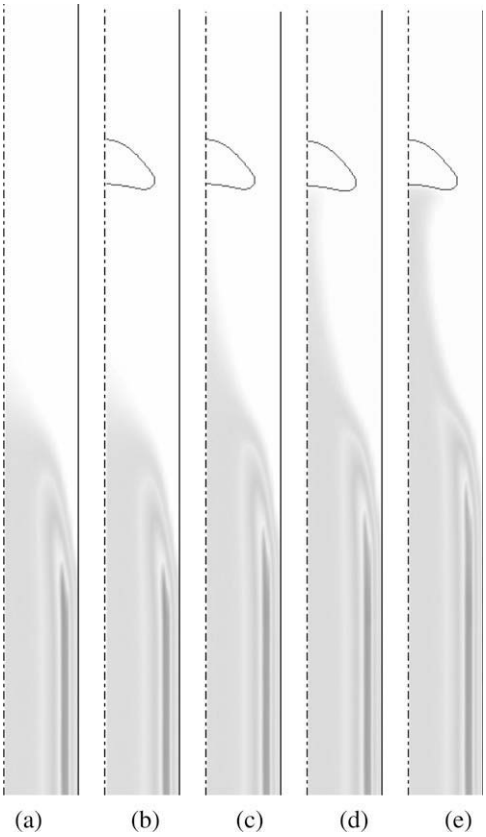

Fig. 9. The shape of the large bubble and volume fraction field of phase 3 at different values of L at time 0.3 s: (a) ∞, (b) 25 mm, (c) 18 mm, (d) 15 mm, (e) 10 mm.

bottom of computational domain. At initial time there is a domain, downstream of the large bubble, filled with small bubbles. The computed volume fraction profile under experimental condition 1 shown in Section 5.2 is chosen as the initial profile in the domain filled with small bubbles as well as at the inlet of the computational domain. The initial velocity profile of each phase in cross sections is set as the corresponding computed profile under experimental condition 1. The top of the computational domain is set as outlet, the left side is set as the centerline of the pipe, i.e., the symmetric axis of pipe, and the right side as the wall of the pipe.

The properties of the liquid and the gas, such as density and viscosity, are the same as those in Section 5.2. The surface tension is 0.0465 N/m.

In general the movement and deformation of the interface of the large bubble is simulated with the VOF method and the movement of single fluid or bubbly flow is calculated with the two-fluid model. The two cases are included in the proposed model. The implementation of the proposed model can satisfy both of the two cases in a unified framework. The total simulation time is 0.3 s, which is enough to show the stable shape of the large bubble and the behaviour of the interactions of the large bubble and the following small bubble swarms.

Define the variable L as the distance from the bottom of the hemisphere shaped large bubble to the top of the domain filled with bubbly flow at initial time, as shown in Fig. 8. Five cases of $L = \infty$, 25 mm, 18 mm, 15 mm and 10 mm are simulated as shown in Fig. 9. The denotation ∞ means the absence of large bubble. The result in the case of "∞" is the benchmark with which the other four cases are compared to study the interactions of the large bubble and swarm of small bubbles.

Fig. 10 shows the velocity field near the large bubble when L = 10 mm. When the large bubble is rising, the liquid near the

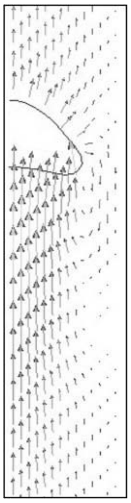

Fig. 10. The velocity field of liquid phase near the large bubble with L = 10 mm at time 0.3 s.

bubble head is pushed forward and away from the centerline and starts to fall around the large bubble. Then the liquid plunges into the wake zone of the large bubble, and a recirculation zone in the wake of the large bubble is clearly seen. The velocity field near the large bubble in the other cases are almost the same as that in the case of L = 10 mm. In Fig. 9, darker colour represents the domain with higher volume fraction of small bubbles. It can be seen from Fig. 9 that with decreased L, i.e., the large bubble are closer to small bubbles at initial time, more small bubbles are cycloned into the tail of the large bubble. Compared to the cases of $L = \infty$ and L = 25 mm, it is observed that the movement and phase profiles of small bubbles in the two cases are almost the same. However, there are more or less some small bubbles cycloned by the

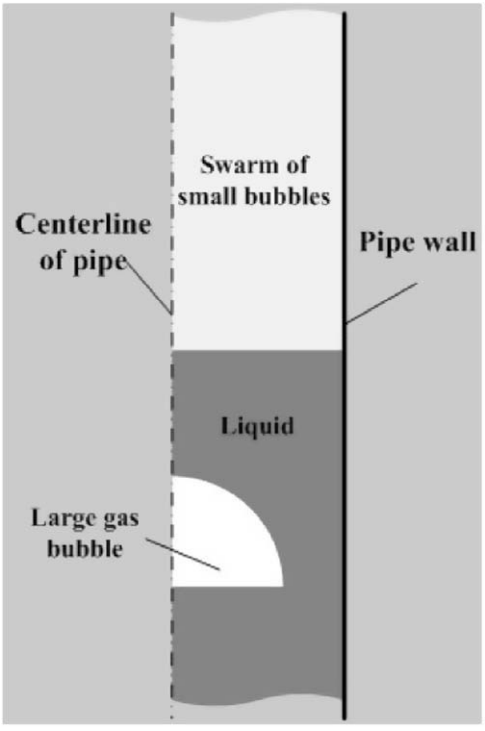

Fig. 11. The schematic diagram of computational domain at initial time in Section 5.4.

recirculation in the wake of the large bubble in the other cases. Thus, it is concluded that there is a threshold value of L, which determines the interactions between large bubble and swarm of small bubbles. The interactions become more obvious with decreased L, once it is small than the threshold value. From the five cases of Fig. 9, it is can also be seen that the swarm of small bubbles has almost no effect on the movement and deformation of the large bubble. These conclusions are very similar to those of Talvy et al. (2000), though they studied the interactions between the leading bubble and the trailing bubble in the slug flow in a vertical tube.

5.4. Bubbly flow followed by a rising large gas bubble in a vertical pipe

As the final test for the proposed model, a swarm of small bubbles followed by a rising gas bubble with large-length-scale interface are considered. This problem concerns is the effect of the volume addition of the large gas bubble when some small bubbles enters the large gas bubble. The interactions between the large bubble and the small bubbles as well as the mass exchange between them are simulated.

A two-dimensional coordinate system assuming axial symmetry about the centerline of the pipe is employed. The radius of the pipe is 14 mm the grid sizes in x- and y-directions are equal and specified as 0.001 mm. The initial shape of the large gas bubble is a hemisphere with a radius of 9 mm. The initial shape has no effect on the computed results. There is a zone, which is upstream of the large bubble, is filled with the swarm of small bubbles with uniform volume fraction at initial time, as shown in Fig. 11. The other zone is occupied by liquid. Note that only the drag force between the small bubbles and the surrounding liquid is considered and other interactions such as lift force and wall force are ignored for simplicity. The initial velocity profile of phase 1 and phase 3 in cross sections is set as the corresponding computed profiles under experimental condition 1 in the Section 5.2. The total simulation time is 1.5 s, which is long enough to show the interactions between the large bubble and the following small bubbles and the mass exchange between them. The pipe should be long enough to satisfy the movement of the large bubble and the small bubbles during the time span of 1.5 s.

In this problem, the density of fluid is 866 kg/m^3 and the density of gas is 1.0 kg/m^3. The viscosity of fluid is 0.06 Pa s. The surface tension is 0.12 N/m.

The large gas bubble rises along the centerline of the pipe. Finally a steady bubble shape will be formed. A recirculation zone in the wake of the large gas bubble is developed. The small bubbles and the liquid near the large gas bubble are pushed to the pipe wall and then plunge into the wake of the large bubble. Part of the small

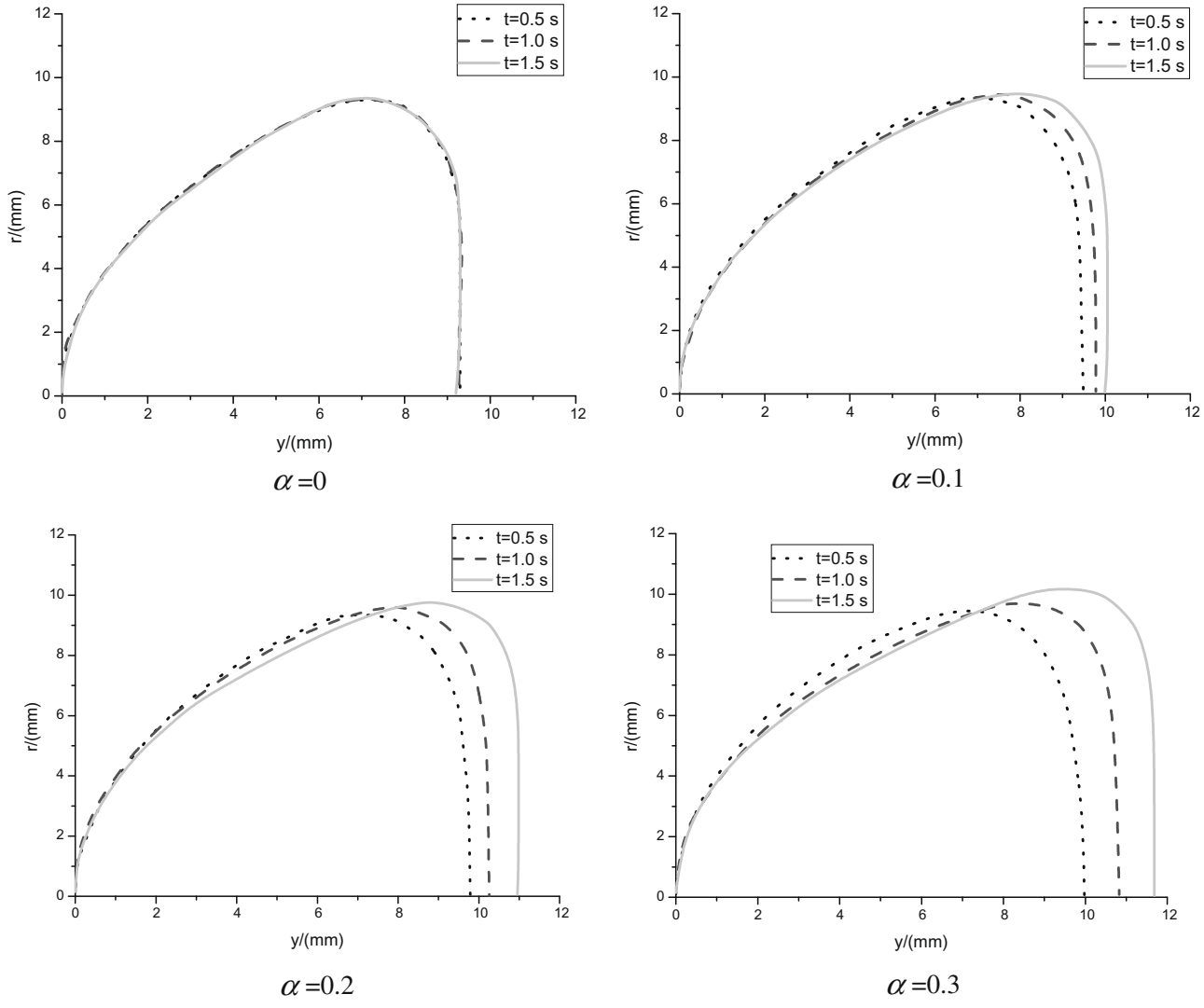

Fig. 12. (a) Comparison of the computed shapes of the large gas bubble at different time steps with the same value of α. (b) Comparison of the computed shapes of the large gas bubble at different values of α at the same time step.

bubbles rush directly into the wake zone behind the recirculation zone. The other small bubbles return to the large gas bubble due to recirculation and coalesce with it.

Denote α as the volume fraction of phase 3 in the small bubble domain at initial time. Liu and Bankoff (1993) have investigated the air–water bubbly flow pattern in a vertical pipe, and found that the volume fraction is below 0.35. Many dispersed bubbles will coalesce into large bubbles when the volume fraction is above 0.35, i.e., the flow pattern is changed. Thus, $\alpha = 0$, 0.1, 0.2 and 0.3 are selected for simulation the case of $\alpha = 0$ is regarded as the benchmark since there is no mass exchange between the small bubbles and the large gas bubble.

In actual situation, the coalescences among small bubbles indicated by phase 3 may happen when the value of α is very high. This kind of coalescences can generate the bubbles with interfaces of larger length scale. The larger bubbles can be classified as phase 2. However, this kind of coalescences among phase 3 are out of consideration in this test. Although many attempts have been made, it is still a difficult work to describe the transition of the phase 3 to phase 2 through numerical techniques when this kind of coalescences happen. Moreover, how the criterion on the transition of the phase 3 with large volume fraction to phase 2 is determined needs further study.

The shapes of the large gas bubble with different values of α at different time steps are shown in Fig. 12. In Fig. 12a, the shapes of the large gas bubble at t = 0.5 s, 1.0 s and 1.5 s with the same value of α are shown. Take the case of $\alpha = 0.2$ as an example. With time processing, the volume of the large gas bubble becomes larger as some small bubbles are furled in to the recirculation zone and enter the large gas bubble. For the case of $\alpha = 0$, the volumes of the large gas bubble at three different time steps are kept unchanged and the shapes are almost the same, since no small bubble coalesces into the large gas bubble. In Fig. 12b, the shapes of the large gas bubble at $\alpha = 0$, 0.1, 0.2 and 0.3 at the same time step are shown. It can be seen that with the increased value of α the larger volume of the large gas bubble is attained at the same time step, since more small bubbles enter the large gas bubble.

It is noted that for the last two tests the two test configurations are hard to realize in experiment. In fact, the flows with both large-length-scale interfaces and small-length-scale interfaces are very common in experiment and many experimental data have been obtained. However, most of these flows contain various coalescences and breakups that are too complex and beyond the present capability of simulation. In spite of no experimental data for comparison, the merits of the proposed model have still been shown in the last two tests.

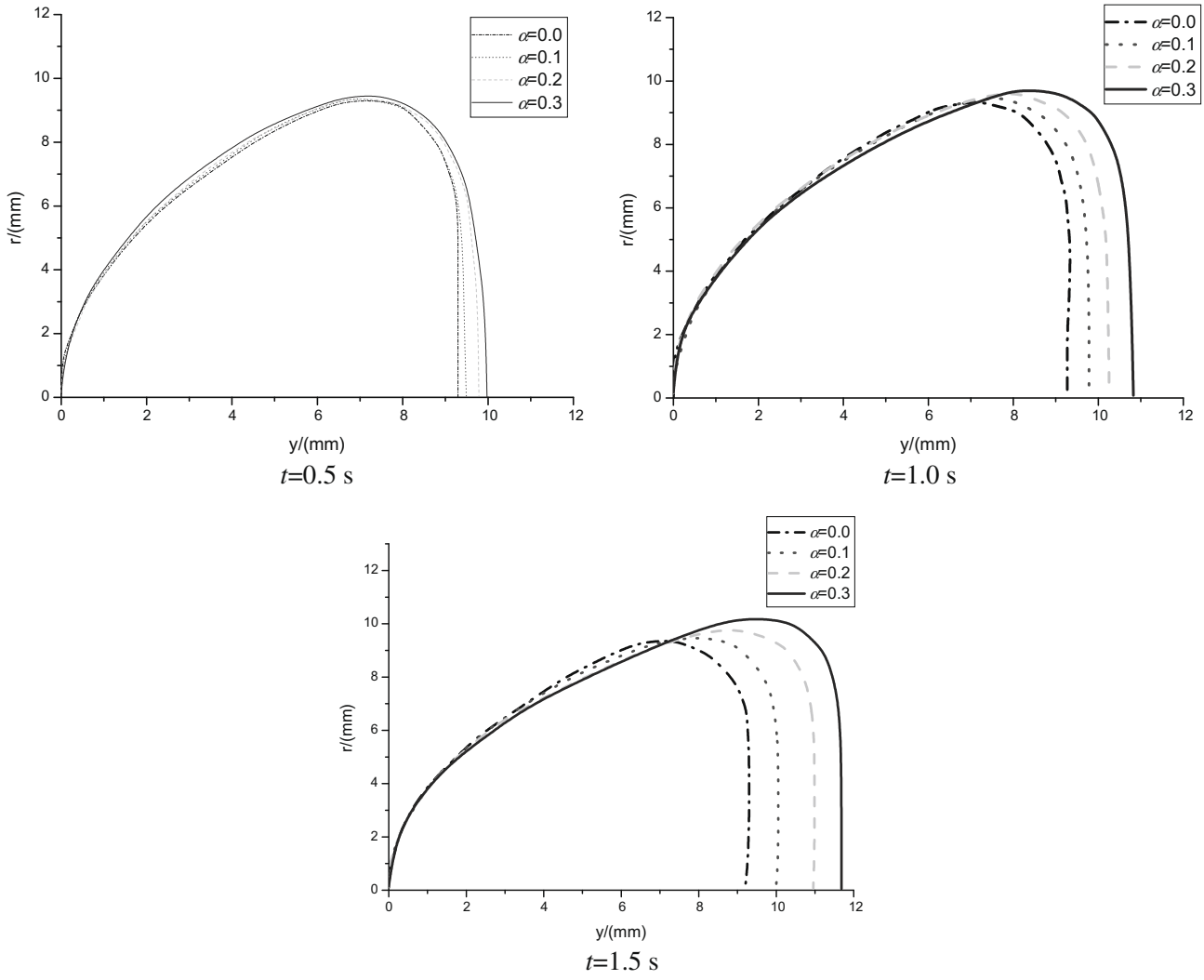

Fig. 12 (*continued*)

6. Conclusion

In this paper, a new model for multiphase flow coupling two basic models, the model based on interface tracking method and the two-fluid model, has been proposed and used for the simulation of incompressible gas–liquid two-phase flow. The proposed model is characterized by the capability of simulating the gas–liquid two-phase flow with complex flow patterns, for example, the flow in which both large-length-scale interface and small-length-scale interface coexist.

The proposed model possesses all the characteristics of the two basic models and can be reduced to either of the two models. The transition between the two basic models is a "natural" process in the unified solution framework. One weakness of this model is that the conservation of phase 1 and 3 cannot be guaranteed in the zone where all three phases coexist, which is the cost of considering the particularity of phase 2. However, it has a negligible influence on the final calculation results.

Four problems are provided to show the main merits of the proposed model. The first two problems show the equivalence of the proposed model to the two basic models, which are the two extreme cases of the proposed model. The last two ones show the capability of simulating the flow containing both large-length-scale interfaces and small-length-scale interfaces, which is closer to real flow conditions, along with the interactions between them.

In the proposed model, flows are divided into three phases, i.e., the liquid phase, the large-length-scale-interface phase (LSI phase) and the small-length-scale-interface phase (SSI phase). The division considering length scale of interface becomes the basis of implementing the proposed model. Building the unified solution framework shared by the two basic models is a critical work for the new model, because it makes sure that the two basic models are solved with the same algorithm. The special treatment of "volume fraction redistribution" is implemented through the derivation of the proposed model. The treatment deals with the connection between the two basic models within the unified solution framework. The volume addition due to some portion of SSI phase coalescing into LSI phase is also considered with another special treatment. Since the volume fraction of the LSI phase is required to be capable of not only keeping its physical meaning but also indicating the location of the large-length-scale interface, the VOF method is selected to advect the large-length-scale interface. Based on the unified solution framework, the modified MCBA–SIMPLE algorithm is employed to solve the governing equations, where the pressure-correction equations are derived not by continuity equation of single phase but by the modified global mass conservation equation of all phases. One of the merits of the MCBA–SIMPLE algorithm, i.e., it can extend many other techniques developed for single-fluid flow to multiphase flow, is also implanted in the proposed model. The merit and the solution framework of the MCBA–SIMPLE algorithm guarantee the proposed model to be an open system and to be adapted to other complex situations met in engineering.

Acknowledgement

The financial support from Natural Science Fund of China (10372077) is gratefully acknowledged.

Appendix A

The MCBA–SIMPLE algorithm (Darwish et al., 2001) is an extension of the single-phase SIMPLE algorithm to multi-phase flows. In the algorithm, in order to derive the pressure-correction equation, the mass conservation equations of various phases are added to yield the global mass conservation equation given by

$$\sum_k \left\{ \frac{(\alpha_k\rho_k) - (\alpha_k\rho_k)^{\text{old}}}{\delta t}\delta V + \Delta(\alpha_k\rho_k\vec{\boldsymbol{U}}_k\cdot\vec{\boldsymbol{S}}) \right\} = 0 \tag{A.1}$$

where the subscript "k" means the phase of k and the Δ operator represents the operation

$$\Delta(\Theta) = \sum_{f=\text{NB}} \Theta_f \tag{A.2}$$

and $\vec{\boldsymbol{S}}$ are the surface vector at cell face.

The SIMPLE algorithm consists of two stages, the predictor stage and the corrector stage. In the predictor stage, with solving the momentum equations, the resulting velocity field, denoted by $\vec{\boldsymbol{U}}_k^*$, now satisfies the momentum equations. However, it will not, in general, satisfy the mass conservation equations. Thus, the corrector stage is needed in order to yield the velocity and pressure fields satisfying both momentum equations and mass conservation equations. With denoting the corrections for pressure and velocity fields by p' and $\vec{\boldsymbol{U}}_k'$, respectively, the two corrected fields are given by

$$p = p^o + p', \quad \vec{\boldsymbol{U}}_k = \vec{\boldsymbol{U}}_k^* + \vec{\boldsymbol{U}}_k' \tag{A.3}$$

where the superscript "o" refers to the values of the previous iteration or the guessed ones.

In the predictor stage, the fields of $\vec{\boldsymbol{U}}_k^*$ and p^o satisfy the momentum equations given by

$$A_k\vec{\boldsymbol{U}}_k^* = \sum_{\text{NB}} A_{k,\text{NB}}\vec{\boldsymbol{U}}_{k,\text{NB}}^* + \vec{\boldsymbol{B}}_k - \alpha_k\delta V\nabla p^o \tag{A.4}$$

where $\vec{\boldsymbol{B}}_k$ means body force vector per unit volume of fluid k.

The above equation can be rewritten as

$$\vec{\boldsymbol{U}}_k^* = \frac{\sum_{NB} A_{k,\text{NB}}\vec{\boldsymbol{U}}_{k,\text{NB}}^* + \vec{\boldsymbol{B}}_k}{A_k} - \alpha_k D_k\nabla p^o \tag{A.5}$$

where $D_k = \frac{\delta V}{A_k}$.

While the final solutions can be written, in the form of the above equation, as

$$\vec{\boldsymbol{U}}_k = \frac{\sum_{NB} A_{k,\text{NB}}\vec{\boldsymbol{U}}_{k,\text{NB}} + \vec{\boldsymbol{B}}_k}{A_k} - \alpha_k D_k\nabla p \tag{A.6}$$

By subtracting the above two sets of equations from each other, the following equation involving the corrected terms is given by

$$\vec{\boldsymbol{U}}_k' = \frac{\sum_{NB} A_{k,\text{NB}}\vec{\boldsymbol{U}}_{k,\text{NB}}'}{A_k} - \alpha_k D_k\nabla p' \tag{A.7}$$

Neglecting the correction to neighboring cells, the above equation reduces to

$$\vec{\boldsymbol{U}}_k' = -\alpha_k D_k\nabla p' \tag{A.8}$$

Moreover, the corrected velocity fields will satisfy the global mass conservation equation. Substituting Eq. (A.7) and $\boldsymbol{U}_k = \boldsymbol{U}_k^* + \boldsymbol{U}_k'$ into Eq. (A.1) and rearranging give the pressure correction equation shown as

$$\sum_k \left\{ \Delta(\alpha_k\rho_k\alpha_k D_k\nabla p'\cdot\vec{\boldsymbol{S}}) \right\} = \sum_k \left\{ \frac{(\alpha_k\rho_k) - (\alpha_k\rho_k)^{\text{old}}}{\delta t}\delta V + \Delta(\alpha_k\rho_k\vec{\boldsymbol{U}}_k^*\cdot\vec{\boldsymbol{S}}) \right\} \tag{A.9}$$

The correction to pressure field p' is achieved when solving the set of pressure correction equations. Then the correction is applied to pressure and velocity fields using the following equations:

$$p^{\text{new}} = p^{o} + p', \quad \vec{\boldsymbol{U}}_k^{\text{new}} = \vec{\boldsymbol{U}}_k^{*} - \alpha_k D_k \nabla p' \tag{A.10}$$

where the superscript "new" refers to the initial values of the next iteration.

Numerical experiments using the above approach to simulate air–water-like flows have shown poor conservation of the lighter fluid (Darwish et al., 2001). In the air–water-like flows, a high density difference between weightier fluid and lighter fluid is present, which makes the contribution of weightier fluid to global mass conservation equation much larger than that of lighter fluid. The pressure correction will, to a great extent, tend to drive the weightier fluid to conservation, while the lighter fluid can be neglected. The problem can be considerably alleviated by normalizing the individual mass conservation equations, and hence the global mass conservation equation, by means of a weighting factor such as a reference density ρ_k (Darwish et al., 2001). Therefore, the pressure correction equation can be modified as follows:

$$\sum_k \left\{ \frac{\Delta(\alpha_k \rho_k \alpha_k D_k \nabla p' \cdot \vec{\boldsymbol{S}})}{\rho_k} \right\} = \sum_k \left\{ \frac{(\alpha_k \rho_k) - (\alpha_k \rho_k)^{\text{old}}}{\delta t \cdot \rho_k} \delta V + \frac{\Delta(\alpha_k \rho_k \vec{\boldsymbol{U}}_k^{*} \cdot \vec{\boldsymbol{S}})}{\rho_k} \right\}$$

which can be rearranged and given by

$$\sum_k \{\Delta(\alpha_k \alpha_k D_k \nabla p' \cdot \vec{\boldsymbol{S}})\} = \sum_k \left\{ \frac{\alpha_k - \alpha_k^{\text{old}}}{\delta t} \delta V + \Delta(\alpha_k \vec{\boldsymbol{U}}_k^{*} \cdot \vec{\boldsymbol{S}}) \right\} \tag{A.11}$$

Here the assumption of incompressibility of fluids is used.

References

Anglart, H., Podowski, M.Z., 2002. On the multidimensional modeling of gas–liquid slug flows. In: Proceedings of the 12th International Heat Transfer Conference, Grenoble, France.

Antal, S.P., Lahey, J.R., Flaherty, J.E., 1991. Analysis of phase distribution in fully developed laminar bubbly two-phase flow. Int. J. Multiphase Flow 17, 635–652.

Bhaga, D., Weber, M.E., 1981. Bubbles in viscous liquids: shapes, wakes and velocities. J. Fluid Mech. 105, 61–85.

Brackbill, J.U., Kothe, D.B., Zemach, C., 1992. A continuum method for modeling surface tension. J. Comput. Phys. 100, 335–354.

Bruce, S.H., Wendroff, B., 1984. Two-phase flow: models and methods. J. Comput. Phys. 56, 363–409.

Cerne, G., Petelin, S., Tiselj, I., 2001. Coupling of the interface tracking and the two-fluid models for the simulation of incompressible two-phase flow. J. Comput. Phys. 171, 776–804.

Darwish, M., Moukalled, F., Sekar, B., 2001. A unified formulation of the segregated class of algorithms for multifluid flow at all speeds. Numer. Heat Transfer B: Fundam. 40, 99–137.

Drew, D.A., 1983. Mathematical modeling of two-phase flow. Annu. Rev. Fluid Mech. 15, 261–291.

Drew, D.A., Lahey, R.T., 1979. Application of general constitutive principles to the derivation of multidimensional two-phase flow equations. Int. J. Multiphase Flow 5, 243–264.

Drew, D.A., Lahey, R.T., 1982. Phase-distribution mechanisms in turbulent low-quality two-phase flow in a circular pipe. J. Fluid Mech. Digital Arch. 117, 91–106.

Drew, D., Passman, S., 1998. Theory of Multicomponent Fluids. Springer, New York.

Gardner, C.L., Glimm, J., McBryan, O., Menikoff, R., Sharp, D.H., Zhang, Q., 1988. The dynamics of bubble growth for Rayleigh–Taylor unstable interfaces. Phys. Fluids 31, 447–465.

Grace, J.R., 1973. Shapes and velocities of bubbles rising in infinite liquids. Chem. Eng. Res. Des. 51, 116–120.

Gueyffier, D., Li, J., Nadim, A., Scardovelli, R., Zaleski, S., 1999. Volume-of-fluid interface tracking with smoothed surface stress methods for three-dimensional flows. J. Comput. Phys. 152, 423–456.

Harlow, F.H., Welch, J.E., 1965. Numerical calculation of time-dependent viscous incompressible flow of fluid with free surface. Phys. Fluids 8, 2182–2189.

Hirt, C.W., Nichols, B.D., 1981. Volume of fluid (VOF) method for the dynamics of free boundaries. J. Comput. Phys. 39, 201–225.

Hirt, C.W., Amsden, A.A., Cook, J.L., 1974. An arbitrary Lagrangian–Eulerian computing method for all flow speeds. J. Comput. Phys. 14, 227–253.

Hnat, J.G., Buckmaster, J.D., 1976. Spherical cap bubbles and skirt formation. Phys. Fluids 19, 182–194.

Hughes, T.J., Liu, W.K., Zimmermann, T.K., 1981. Lagrangian–Eulerian finite element formulation for incompressible viscous flows. Comput. Method Appl. Mech. Eng. 29, 329–349.

Ishii, M., 1975. Thermo-Fluid Dynamic Theory of Two-Phase Flow. Eyrolles, Paris.

Ishii, M., Mishima, K., 1984. Two-fluid model and hydrodynamic constitutive relations. Nucl. Eng. Des. 82, 107–126.

Ishii, M., Zuber, N., 1979. Drag coefficient and relative velocity in bubbly, droplet or particulate flows. AIChE J. 25, 843–855.

Lamb, H., 1932. Hydrodynamics. Cambridge University Press, New York.

Liu, T.J., Bankoff, S.G., 1993. Structure of air–water bubbly flow in a vertical pipe—I. Liquid mean velocity and turbulence measurements. Int. J. Heat Mass Transfer 36, 1049–1060.

Lopez de Bertodano, M.A., 1992. Turbulent bubbly two-phase flow in a triangular duct. Ph.D. dissertation, Rensselaer Polytechnic Institute, New York.

Moraga, F.J., Bonetto, F.J., Lahey, R.T., 1999. Lateral forces on spheres in turbulent uniform shear flow. Int. J. Multiphase Flow 25, 1321–1372.

Moukalled, F., Darwish, M., Sekar, B., 2003. A pressure-based algorithm for multi-phase flow at all speeds. J. Comput. Phys. 190, 550–571.

Nigmatulin, R.I., 1979. Spatial averaging in the mechanics of heterogeneous and dispersed systems. Int. J. Multiphase Flow 5, 353–385.

Ohta, M., Imura, T., Yoshida, Y., Sussman, M., 2005. A computational study of the effect of initial bubble conditions on the motion of a gas bubble rising in viscous liquids. Int. J. Multiphase Flow 31, 223–237.

Olsson, E., Kreiss, G., 2005. A conservative level set method for two phase flow. J. Comput. Phys. 210, 225–246.

Puckett, E.G., Almgren, A.S., Bell, J.B., Marcus, D.L., Rider, W.J., 1997. A high-order projection method for tracking fluid interfaces in variable density incompressible flows. J. Comput. Phys. 130, 269–282.

Sato, Y., Sadatomi, M., Sekoguchi, K., 1981. Momentum and heat transfer in two-phase bubble flow—I. Theory. Int. J. Multiphase Flow 7, 167–177.

Sethian, J.A., 1998. Level Set Methods. Cambridge University Press, Cambridge, UK.

Song, Q., Luo, R., Yang, X.Y., Wang, Z., 2001. Phase distributions for upward laminar dilute bubbly flows with non-uniform bubble sizes in a vertical pipe. Int. J. Multiphase Flow 27, 379–390.

Sussman, M., Almgren, A.S., Bell, J.B., Colella, P., Howell, L.H., Welcome, M.L., 1999. An adaptive level set approach for incompressible two-phase flows. J. Comput. Phys. 148, 81–124.

Talvy, C.A., Shemer, L., Barnea, D., 2000. On the interaction between two consecutive elongated bubbles in a vertical pipe. Int. J. Multiphase Flow 26, 1905–1923.

Tomiyama, A., Zun, I., Higaki, H., Makino, Y., Sakaguchi, T., 1997. A three-dimensional particle tracking method for bubbly flow simulation. Nucl. Eng. Des. 175, 77–86.

Unverdi, S.O., Tryggvason, G., 1992. A front-tracking method for viscous, incompressible, multi-fluid flows. J. Comput. Phys. 100, 25–37.

Wallis, G.B., 1969. One-Dimensional Two-Phase Flow. McGraw-Hill, New York.

Xu, Z., 2004. Theoretical and experimental investigations on quasi-laminar viscous bubbly flows. Ph.D. dissertation, Tsinghua University, Bei Jing.

Zhang, D.Z., Prosperetti, A., 1994. Ensemble phase-averaged equations for bubbly flows. Phys. Fluids 6, 2956.

Zheng, D., He, X., Che, D., 2007. CFD simulations of hydrodynamic characteristics in a gas–liquid vertical upward slug flow. Int. J. Heat Mass Transfer 50, 4151–4165.